Available online at www.sciencedirect.com

ScienceDirect

Scripta Materialia 101 (2015) 28–31

Scripta MATERIALIA

www.elsevier.com/locate/scriptamat

High-speed extrusion of heat-treatable Mg–Al–Ca–Mn dilute alloy

T. Nakata,[a,*] T. Mezaki,[a] R. Ajima,[a] C. Xu,[a] K. Oh-ishi,[a] K. Shimizu,[b] S. Hanaki,[b] T.T. Sasaki,[c] K. Hono[c] and S. Kamado[a]

[a]*Nagaoka University of Technology, 1603-1, Kamitomioka, Nagaoka 940-2188, Japan*
[b]*Sankyo Tateyama, Inc. Sankyo Material-Company, 8-3, Nagonoe, Imizu, Toyama 934-8515, Japan*
[c]*National Institute for Materials Science, 1-2-1, Sengen, Tsukuba 305-0047, Japan*

Received 8 September 2014; revised 16 January 2015; accepted 17 January 2015
Available online 4 February 2015

Abstract—A newly developed dilute magnesium alloy, Mg–0.27Al–0.13Ca–0.21Mn (at.%), shows extraordinary high-speed extrudability of a die-exit speed of 60 m/min. Subsequent artificial aging at 200 °C (T5) enhanced the proof stress from 170 MPa to 207 MPa due to the precipitation of Guinier Preston (G.P.) zones and weakened basal texture while keeping good ductility of 12.5%. High-speed extrusion reduces the processing cost, so the dilute Mg–Al–Ca–Mn alloy could be an industrially viable low-cost medium strength structural material.

Keywords: High-speed extrusion; Mg–Al–Ca–Mn alloy; Age hardening; Tensile properties

Wrought magnesium alloys have great potential as light-weight structural materials for weight reduction of transportation vehicles to improve their fuel efficiencies. However, practical use of magnesium alloys is limited due to their poor workability and low strengths. For instance, a conventional magnesium alloy, AZ31, can be extruded at up to 15 m/min, which shows low 0.2% proof stress of about 165 MPa [1]. Recently, Murai and Davis [1–3] reported that the extrusion speed of magnesium alloys can be increased by lowering the contents of alloying elements. However, the Mg–0.5Al–0.25Zn–0.1Mn (wt.%) alloy extruded at 30 m/min exhibits insufficient 0.2% proof stress of 180 MPa [2], and post-extrusion strengthening by aging is not possible because all the alloying elements are completely soluble into α-Mg as a solid solution at room temperature. On the other hand, Mg–0.3Al–0.5Ca (wt.%) alloy, in which Ca and Al have larger and smaller atomic radii than Mg with a large negative mixing enthalpy, exhibits notable age-hardening response due to the precipitation of monolayer ordered Guinier Preston (G.P.) zones lying on the basal plane [4,5]. Considering these results, we anticipate improvements in both workability and strengths by using Mg–Al–Ca and Mg–Zn–Ca dilute alloys. This paper reports a successful high-speed extrusion of a newly developed Mg–0.27Al–0.13Ca–0.21Mn (at.%) or Mg–0.30Al–0.21Ca–0.47Mn (wt.%) (AXM0301502) dilute alloy and subsequent precipitation hardening by a T5 heat-treatment.

All alloy ingots were prepared by direct-chill (DC) casting. The chemical compositions of the alloys are summarized in Table 1 in both at.% and wt.%. For comparison, DC-cast AZ31 alloy, a standard commercial wrought magnesium alloy, was also used. A differential scanning calorimeter (DSC) was used for determining of homogenization temperatures prior to extrusion and the AXM0301502 alloy was homogenized at 500 °C for 24 h in an argon atmosphere, followed by water quenching. For the AZ31 alloy, a homogenization treatment was performed at 415 °C for 24 h. Then, the alloy was additionally homogenized at 500 °C for 24 h. Both homogenized alloys were extruded using an indirect extrusion method. Table 2 shows the extrusion conditions performed in this study. The extruded AXM0301502 and AZ31 alloys were artificially aged at 200 °C; age-hardening responses were measured by a Vickers hardness tester (VMT-7S) from seven individual indentations under a load of 9.8 N on the plane perpendicular to the extrusion direction. Mechanical properties were evaluated by tensile test at room temperature with an initial strain rate of 10^{-3} s^{-1} along the extrusion direction. The tensile test specimens were 4 mm in diameter and 22 mm in gage length. Microstructures were characterized by electron backscattered diffraction (EBSD) with 2 μm of step size using a JSM-7000F scanning electron microscope (SEM) and an Orientation Imaging Microscopy software, and a JEM-2100F transmission electron microscope (TEM).

Figure 1 shows the processing charts applied to AXM0301502 and AZ31 alloys and the appearance of the surfaces of the bars extruded at a die-exit speed of

* Corresponding author.; e-mail: s123055@stn.nagaokaut.ac.jp

http://dx.doi.org/10.1016/j.scriptamat.2015.01.010
1359-6462/

Table 1. Chemical compositions of alloy ingots [at.% (wt.%)].

Alloy	Al	Ca	Mn	Zn	Mg
AXM0301502	0.27 (0.30)	0.13 (0.21)	0.21 (0.47)	–	Bal.
AZ31	2.70 (2.97)	–	0.16 (0.36)	0.30 (0.80)	Bal.

Table 2. Conditions of indirect extrusion.

Alloy	Temperature [°C]	Die-exit speed [m/min]	Extrusion ratio
AXM0301502	500	60	20
AZ31		1.2, 12, 60	

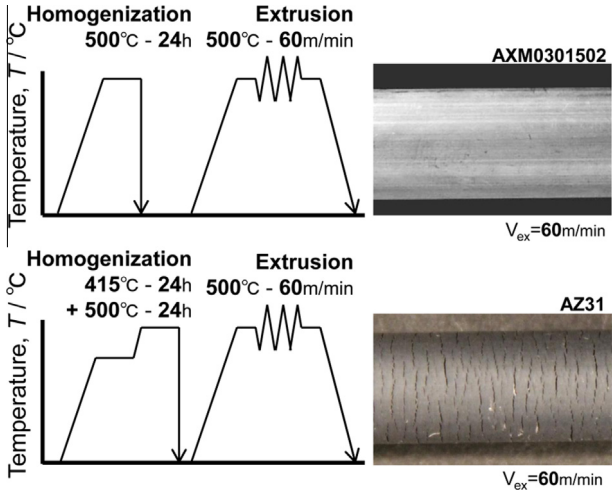

Figure 1. Processing charts applied to AXM0301502 and AZ31 alloys and the appearance of the surface of the bars extruded at the die-exit-speed of 60 m/min at 500 °C. Note that the two-step heat treatment was required to homogenize the AZ31 alloy due to the presence of nonequilibrium $Mg_{17}Al_{12}$ phase crystalizing at 438 °C and solute segregation of Al and Zn in as-cast AZ31 alloys [6], while only one-step homogenization treatment is required for AXM0301502 alloy.

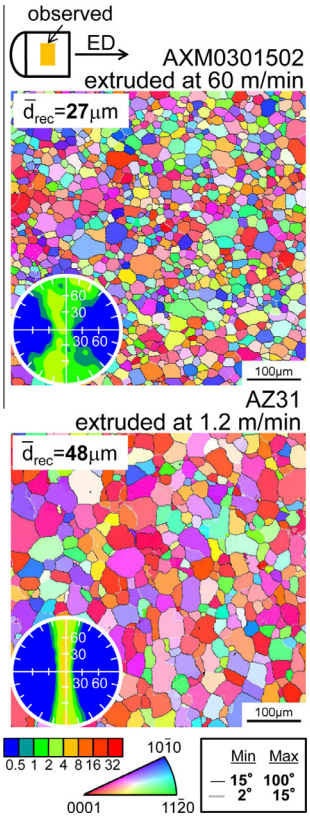

Figure 2. Inverse pole figure maps and (0001) pole figures of AXM0301502 and AZ31 alloys extruded at 500 °C at die-exit speeds of 60 and 1.2 m/min, respectively.

60 m/min at 500 °C. While the AXM0301502 sample can be homogenized in one step at 500 °C, the AZ31 had to be homogenized in two steps because as-cast AZ31 alloy has nonequilibrium $Mg_{17}Al_{12}$ (β) phase crystalizing at 438 °C and solute segregation of Al and Zn at grain boundaries [6]. The AXM0301502 alloy shows a crack-free surface even at the die-exit speed of 60 m/min, while the AZ31 alloy shows many surface cracks perpendicular to the extrusion direction. In addition, the AZ31 alloy shows gray surface, suggesting a particle melting oxidation of the Mg matrix because of the friction heat during extrusion. The AZ31 alloy showed metallic shiny surface only when it was extruded at the die-exit rate of 1.2 m/min. In general, high content alloys with a low-melting-point eutectic structure or with a low solidus temperature tend to show surface cracking during extrusion [3,6]. Because of this, good surface quality was not obtained in the AZ31 alloy extruded at extrusion rates faster than 12 m/min in this study. On the other hand, the homogenized AXM0301502 alloy does not contain any low-melting-point eutectic structure and the solidus temperature (610 °C) is much higher than that of AZ31 (570 °C [7]). Also the Ca retards oxidation during heating. As a result, high-speed extrusion of 60 m/min was possible for the homogenized AXM0301502 alloy keeping the good surface quality. Since the AZ31 alloy was extrudable at the die-exit speed of 1.2 m/min, hereafter the microstructures of the AXM0301502 alloy extruded at 60 m/min and the AZ31 alloy extruded at 1.2 m/min are compared.

Figure 2 shows inverse pole figure (IPF) maps and (0001) pole figures (PF) of the AXM0301502 alloy extruded at a die-exit speed of 60 m/min at 500 °C. For comparison, those of the AZ31 alloy extruded at a die-exit speed of 1.2 m/min at 500 °C are also shown. These maps were taken from the center of the plane parallel to the extrusion direction as schematically shown in the figure. The AXM0301502 alloy shows fully recrystallized grains in the whole area. Compared to the AZ31 alloy, the AXM0301502 alloy exhibits finer grain size of 27 μm and weaker basal texture, in which the basal planes are tilted away from the extrusion direction.

Figure 3a shows variations in Vickers hardness values as functions of aging time when the extruded alloys were artificially aged at 200 °C without solution heat treatment. The AXM0301502 alloy reaches a peak hardness in 4 h with a hardness increment of about 7 HV, while the AZ31 alloy

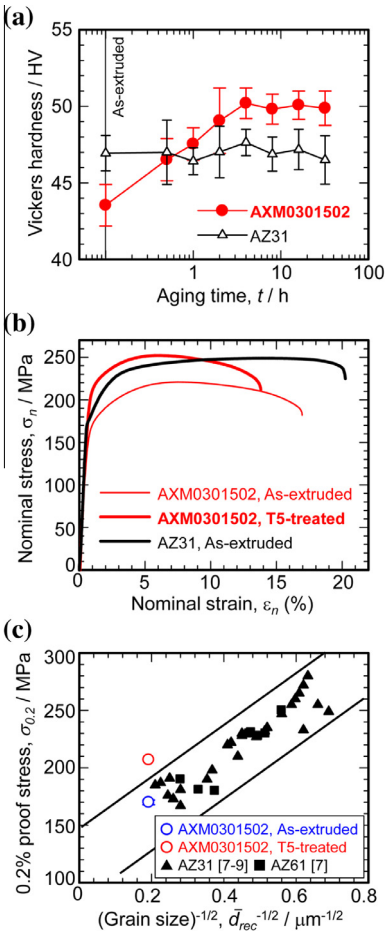

Figure 3. (a) Variations in Vickers hardness values as functions of aging time when the extruded alloys were artificially aged at 200 °C without solution heat treatment, (b) Tensile properties of as-extruded and T5-treated AXM0301502 alloys extruded at the die-exit speed of 60 m/min at 500 °C and the as-extruded AZ31 alloy extruded at a die-exit speed of 1.2 m/min at 500 °C, (c) 0.2% proof stress versus grain sizes of as-extruded and T5-treated AXM0301502 alloy extruded at 500 °C at a die-exit speed of 60 m/min, and as-extruded AZ31 and AZ61 alloys from the other literature [8–10].

exhibits no age-hardening response. So we chose the aging conditions at 200 °C for 4 h for the T5 heat-treatment of the AXM0301502 alloy. Figure 3b shows the tensile properties of the as-extruded and T5-treated AXM0301502 alloys and the as-extruded AZ31 alloy. The as-extruded AXM0301502 alloy shows the 0.2% proof stress of 170 MPa and the total elongation of 15.5%, which are slightly lower than those of the AZ31 alloy, 177 MPa and 20%. However, after the T5 heat-treatment, the 0.2% proof stress of the AXM0301502 alloy was improved up to 207 MPa, exceeding 177 MPa for the as-extruded AZ31 alloy. Figure 3c shows the grain size dependence of the 0.2% proof stress of the AXM0301502 alloys and the results of as-extruded AZ31 and AZ61 alloys taken from literatures [8–10]. Typical Hall–Petch relationship [11–13] was reported for the AZ31 and AZ61 alloys; the 0.2% proof stresses tend to increase with a decrease in the grain sizes. The 0.2% proof stress of the as-extruded AXM0301502 alloy is within the range of the Hall–Petch relationship reported for the AZ31 and AZ61 alloys [8–10]. However, the 0.2% proof stress of the T5-treated AXM0301502 alloy

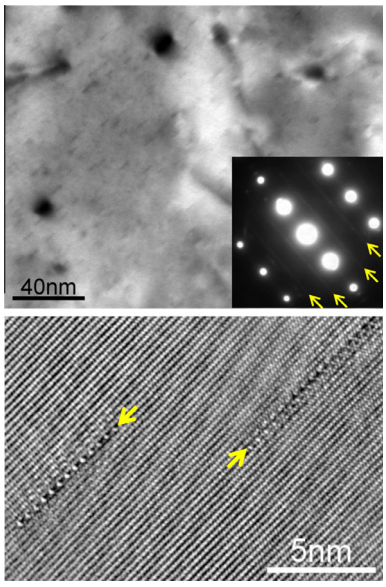

Figure 4. Bright field TEM image, SAED pattern and HRTEM image of T5-treated AXM0301502 alloys extruded at a die-exit-speed of 500 °C at 60 m/min taken from the parallel to [1 0 $\bar{1}$ 0] direction of Mg matrix.

apparently deviates from the general tendency of the proof stress for the AZ31 and AZ61 alloys [8–10]. This suggests that the 0.2% proof stress of the T5-treated AXM0301502 alloy contains a contribution from the precipitation-hardening shown in Figure 3a.

Figure 4 shows a bright-field (BF) TEM image, a selected area diffraction (SAED) pattern, and a high-resolution TEM (HRTEM) image taken from the T5-treated AXM0301502 alloy. The images were recorded with an incident electron beam along the [1 0 $\bar{1}$ 0] zone axis of the Mg matrix. The BF image shows the linear contrast along the trace direction of the basal planes and the SAED pattern shows continuous streaks along the [0 0 0 1] directions as indicated by the arrows, implying the presence of fine plate-like precipitates lying on the basal planes of the Mg matrix with an internal structural order. The precipitates having such features were reported as G.P. zones in Mg–Ca–Al and Mg–Ca–Zn alloys [4,5,14]. From the HRTEM image, the plate-like precipitate is concluded to have a (0 0 0 2) monolayer structure. The composition of this precipitate was reported to be Mg–6Ca–7Al (at.%) in the previous atom probe study [4].

In this work, we have shown that the AXM0301502 alloy could be extruded at an extraordinary die-exit speed of 60 m/min. Considering the upper limit of the die-exit speed of 1.2 m/min for the AZ31 alloy, this extrusion speed is remarkable. The standard extrusion speed of medium strength Al–Si–Mg based 6061 alloys is 50 m/min at 500 °C [3]. Hence, the extrudability of AXM0301502 is superior to that of the medium strength aluminum alloy. This also means that we can use the existing extrusion facilities in aluminum alloy industry for extruding the AXM0301502 alloy. This will reduce the processing cost for the magnesium alloy and makes it competitive with the medium strength aluminum alloys. However, the as-extruded AXM0301502 exhibits lower proof stress than the AZ31 alloy despite the finer grain size in the AXM0301502 alloy (Figs. 2 and 3b). The pole figures in

Figure 2 indicate a stronger basal texture in the AZ31 alloy extruded at the die exit speed of 1.2 m/min. Hence, the higher 0.2% proof stress of the AZ31 alloy can be attributed in part to the contributions of texture-strengthening [6]. In addition, the higher solute content in the AZ31 alloy compared to AXM0301502 causes a higher solution-strengthening in the AZ31 alloy [15]. Unlike the AZ31 alloy, the AXM0301502 alloy shows age-hardening by the T5 heat-treatment; the 0.2% proof stress of the alloy is increased from 170 MPa to 207 MPa by the T5 treatment at 200 °C. Hence, the T5-treated AXM0301502 alloy exhibits higher 0.2% proof stress compared to the AZ31 alloy (Fig. 3b). The high 0.2% proof stress of the T5-treated AXM0301502 alloy is attributed to the precipitation of fine plate-like monolayer G.P. zones on the basal planes of the Mg matrix (Fig. 4). In addition, due to its weakened basal texture, both as-extruded and T5-treated AXM0301502 alloys exhibit relatively good ductilities of 15.5% and 12.5%, respectively.

In summary, high-speed extrusion was successfully applied to a newly developed dilute AXM0301502 alloy. The die-exit speed reaches 60 m/min and the good surface quality is obtained because the homogenized sample is free from low-melting-point eutectic structure and has a high solidus temperature (610 °C). The alloy shows slight age-hardening response by a T5 treatment, which improved the 0.2% proof stress of the high-speed extruded AXM0301502 alloy from 170 MPa to 207 MPa. Because of the weakened basal texture, the T5-treated AXM0301502 alloy shows the relatively good ductility of 12.5%. The mechanical properties as well as the extrudability are superior to commonly used AZ31 alloy. Since major cost for wrought magnesium alloy is attributed to the processing cost, the fast-speed extrudability superior to medium strength aluminum alloys makes this dilute magnesium alloy, AXM0301502, a very attractive, industrially viable structural material.

This work was supported by JSPS Grant-in-Aid for Scientific Research (A) Grant Number 22246094, Grant-in-aid for Scientific Research (B) Grant Number 21360348, and JST, Advanced Low Carbon Technology Research and Development Program (ALCA).

[1] T. Murai, S. Matsuoka, S. Miyamoto, Y. Oki, S. Nagao, H. Sano, J. Jpn. Inst. Light Met. 53 (2003) 27.
[2] T. Murai, J. Jpn. Inst. Light Met. 54 (2004) 472.
[3] C. Davis, M. Barnett, J. Miner. Met. Mater. Soc. 56 (Nov 2004) 22.
[4] J. Jayaraj, C.L. Mendis, T. Ohkubo, K. Oh-ishi, K. Hono, Scripta Mater. 63 (2010) 831.
[5] K. Oh-ishi, R. Watanabe, C.L. Mendis, K. Hono, Mater. Sci. Eng. A 526 (2009) 177.
[6] N. Stanford, D. Atwell, Metall. Mater. Trans. A 44 (2013) 4830.
[7] D.L. Atwell, M.R. Barnett, Metall. Mater. Trans. A 38 (2007) 3032.
[8] J. Bohlen, P. Dobron, J. Swiostek, D. Letzig, F. Chmelik, P. Lukac, K.U. Kainer, Mater. Sci. Eng. A 462 (2007) 302.
[9] Y.N. Wang, C.I. Chang, C.J. Lee, H.K. Lin, J.C. Huang, Scripta Mater. 55 (2006) 637.
[10] Y. Uematsu, K. Tokaji, M. Kamakura, K. Uchida, H. Shibata, N. Bekku, Mater. Sci. Eng. A 434 (2006) 131.
[11] P. Skubisz, T. Skowronek, J. Sinczak, Metall. Found. Eng. 33 (2007) 113.
[12] N. Hansen, Scripta Mater. 51 (2004) 801.
[13] D.J. Jensen, A.W. Thompson, N. Hansen, Metall. Mater. Trans. A 20 (1989) 2803.
[14] J.C. Oh, T. Ohkubo, T. Mukai, K. Hono, Scripta Mater. 53 (2005) 675.
[15] U.F. Kocks, Metall. Trans. A 16 (1985) 2109.